Antioxidant Properties of Pterocarpans through Their Copper(II) Coordination Ability. A DFT Study in Vacuo and in Aqueous Solution†

Giuliano Alagona* and Caterina Ghio*

CNR-IPCF, Institute for Physico-Chemical Processes, MML, Via Moruzzi 1, I-56124 Pisa, Italy

Received: June 12, 2009; Revised Manuscript Received: September 27, 2009

The antioxidant activity of 3,9-dimethoxy-4-prenylpterocarpan (bitucarpin A) and 3,9-dihydroxy-4,8-diprenylpterocarpan (erybraedin C) is supposed to be related to their copper coordination ability. Therefore several complexes with Cu^{2+} of low-energy conformers of these two prenylated pterocarpans, whose conformational landscape was the subject of a prior B3LYP/6-31G* study (Alagona, Ghio, Monti *Phys. Chem. Chem. Phys.* **2004**, *6*, 2849), have been taken into account at the same computational level, with the metal ion described by effective core potentials in the LanL2DZ valence basis set. Their metal ion affinity (MIA) values have been determined and compared with the results obtained earlier with the same methods for the preferred binding sites of plicatin B, a prenylchalcone that can exist in *E* and *Z* configurations as well as in tautomeric forms. The stability order of the metalated species at the various coordination sites strongly depends on their position and nature. The spin density of the cation upon ligand coordination becomes vanishingly small, whereas the ligand spin density approaches 1. Thus the ligand is oxidized to a radical cation ($Ligand^{\bullet+}$), while Cu(II) is reduced to Cu(I). A very favorable MIA is obtained in vacuo when Cu^{2+} is chelated between the prenyl and O lone pair moieties for both pterocarpans (MIA = 370 and 380 kcal/mol for bitucarpin A and erybraedin C, respectively). High affinity values are found also when the cation is sequestered within the two end groups (prenyl π density and D ring) in the O_t configuration (MIA = 371 and 373 kcal/mol for bitucarpin A and erybraedin C, respectively). In aqueous solution, the solvent effect dampens the free energy differences and reduces the MIA especially when the ion is remarkably exposed to the solvent. Conversely, when Cu^{2+} is sequestered, the MIA decrease in solution is limited (MIA = 327 and 360 kcal/mol for bitucarpin A and erybraedin C, respectively). The solvent effect is significantly larger in plicatin B, where the MIA is lowered by 80 to 140 kcal/mol, probably because (a) the screening ability of the substituted phenolic ring is lower and (b) the positive charge on the ligand is less efficiently delocalized than in the four fused ring system of pterocarpans.

I. Introduction

Pterocarpans possessing a 6a,11a-dihydro-6*H*-benzofuro-[3,2-*c*]benzopyran skeleton of cis B/C-ring junction (Chart 1) constitute the second largest group of natural isoflavonoids.[1] Many of them are stress-induced protective agents for plants (phytoalexins), produced in response to the infection caused by fungi, bacteria, or viruses.[1,2] Thus some pterocarpans have antifungal,[3] antitubercular, and estrogenic activity[4] or are antagonists against snake and spider venoms,[5] while others have been reported to inhibit HIV-1 in cell cultures.[6,7] Pterocarpans exhibit interesting antioxidant properties as well, especially low-density lipoprotein (LDL) oxidation inhibitory activities.[8] Since lipoprotein oxidation is crucial in atherogenic processes[9,10] and can be induced by transition metal ions such as copper, the investigation of the structural basis for the ability of active natural compounds to bind Cu^{2+} can help design novel and more potent drugs.

To this end, the Cu(II) sequestering ability of bitucarpin A (3,9-dimethoxy-4-prenylpterocarpan) and erybraedin C (3,9-dihydroxy-4,8-diprenylpterocarpan), whose conformational preferences had been carefully analyzed earlier,[11] taking into account the backbone structure interconversion as well on a model system (*cis* 3,9-dihydroxypterocarpan), is determined in this study. The plicatin B (methyl 3-(4-hydroxy-3-(3-methyl-2-butenyl)phenyl)-2-propenoate) metal ion affinity, evaluated at the same computational level in a previous article,[12] is going to be compared with those of the two pterocarpans. An experimental study[13] on the antioxidant properties of these three natural products under a variety of conditions put forward a number of different explanations for their activity. Our investigation might help discriminate among them.

II. Computational Details

All calculations have been carried out in the density functional theory (DFT) framework making use of the B3LYP hybrid functional[14] and the 6-31G* basis set[15] (pure-d functions) in the gas phase with the Gaussian 03 system of programs.[16] Although the use of relativistic pseudopotentials is not mandatory for Cu^{2+}, with open shell d^9 ground-state electronic configuration, effective core potentials (ECP) that statically include some relativistic effects for the electrons near the nucleus in the LanL2DZ valence basis set[17] have been used for the sake of comparison with previous results. Application of an ECP for Cu(II) was recommended indeed to investigate with B3LYP the variety of structures of Cu(II)−bis(amino acid) complexes.[18] In what follows, B3LYP/6-31G* stands for B3LYP/6-31G*/LanL2DZ even when copper is present for brevity. Spin density distribution was calculated by the Mulliken population analysis

† Part of the "Vincenzo Aquilanti Festschrift".

* Corresponding authors: tel, +39 050 3152450 (Alagona), +39 050 3152449 (Ghio); fax, +39 050 3152442; e-mail, G.Alagona@ipcf.cnr.it and C.Ghio@ipcf.cnr.it.

10.1021/jp905521u
Published on Web 10/15/2009

CHART 1: Structure, Rotatable Bonds, and Numbering of Bitucarpin A, Erybraedin C, and Plicatin B

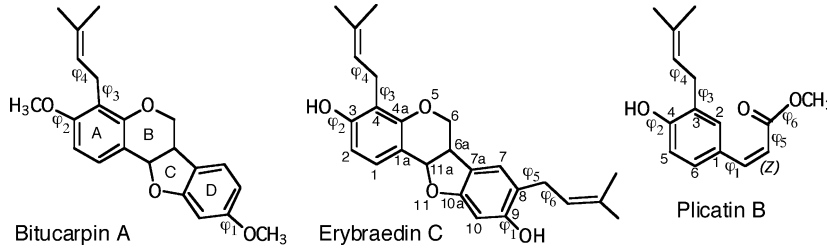

TABLE 1: B3LYP/6-31G* Metal Ion Affinities (kcal/mol) for Few Low-Energy Cu^{2+}−Plicatin B Complexes Computed from Eq 3 (See Text) and Eq 5[d]

complexes[a]	$-\Delta H_{298}$[b]	$-\Delta E_{int}$	E_{def}	MIA[c]
8_PO	316.7	317.5	13.4	330.9
8a_PO	316.5	317.3	17.6	334.8
Z5a_B	337.6	338.6	17.4	356.0
Z5_B	334.1	335.0	15.2	350.3

[a] The isolated plicatin B structure used as reference is followed by the coordination position (PO = prenyl-methoxy O region, B = bridged). [b] Cu^{2+} reference enthalpy = $-195.065696E_h + PV$. [c] Values derived from eq 5 and already reported (among others) in Tables 5 and 7 of ref. 12. [d] The deformation energy (kcal/mol) from eq 4 is also reported.

procedure that coupled with B3LYP produced values closer to the experimental ones.[19]

A variety of attack (or coordination) positions of Cu^{2+} on each stable conformer have been taken into account to evaluate their strength as well as the influence of the ligand internal arrangement on it. The adduct geometries have been fully relaxed to attain the best possible interaction between ligands and metal ion for the processes

$$\text{Ligand} + Cu^{2+} \rightarrow \text{Ligand}\cdots Cu^{2+} \tag{1}$$

The metal ion affinity (MIA) in the *i* complex is usually defined with respect to the global minimum of the ligand[20] as the negative of the enthalpy change ($-\Delta H$) for the ion coordination process

$$\Delta H = H_{[\text{Ligand}\cdots Cu]_i^{2+}} - H_{\text{Ligand}} - H_{Cu^{2+}} \tag{2}$$

This definition, valid for fairly rigid systems, is however devoid of significance for flexible ligands with several distinct minima. As a first attempt to avoid erratic results in our previous study on plicatin B (Plic), the best matching reference structure for the ligand in each complex was located within those optimized for the isolated ligand, $\text{Plic}_{(i,\text{opt})}$, resorting to

$$\Delta H = H_{[\text{Plic}\cdots Cu]_i^{2+}} - H_{\text{Plic}_{(i,\text{opt})}} - H_{Cu^{2+}} \tag{3}$$

The results obtained at 298 K are reported in Table 1 under the header "$-\Delta H_{298}$". In the next column, under the header "$-\Delta E_{int}$", the corresponding values making use of the energy in an equation analogous to eq 3 are reported. Both definitions include, however, the deformation energy of the ligand upon ion binding. The deformation energy is the difference between the energy of the ligand in each complex ($\text{Ligand}_{(i)}$) and that corresponding to its optimized structure ($\text{Ligand}_{(i,\text{opt})}$), that is obtained minimizing the ligand geometry starting from that particular coordination complex, allowing a further refinement of the conformational search

$$E_{\text{def}_{(i)}} = E_{\text{Ligand}_{(i)}} - E_{\text{Ligand}_{(i,\text{opt})}} \tag{4}$$

For flexible ligands, E_{def} is to be subtracted from eqs 2 and 3, suggesting the use of the energy for consistent results.(Of course, it would be possible to refer to the global minimum for computing the MIA making use of the enthalpy, but the deformation energy correction would be anyway carried out using the energy.) Actually E_{def} is contained in $-\Delta E_{int}$, and a possibly analogous value is also in $-\Delta H_{298}$. Therefore, we decided to exploit for the MIA (reported in the last column of Table 1) the negative of the energy change, using as reference structures for the ligand the geometries optimized in each complex

$$\Delta E = E_{[\text{Ligand}\cdots Cu]_i^{2+}} - E_{\text{Ligand}_{(i)}} - E_{Cu^{2+}} \tag{5}$$

because, besides the saving with respect to the high cost of frequency calculations for systems such as the pterocarpans, this definition of the MIA ensures that the greater the computed value the stronger is the affinity. It cannot be used with the enthalpy because the structure of the ligand in the *i* complex, $\text{Ligand}_{(i)}$, is not a stationary point.

The above definitions are consistent with those used in ref 12 for the sake of comparison. The interested readers can find absolute energy values, E_{def}, and MIA in the Supporting Information.

The solvent effect on the complex stability and the total ($G_{tot}(H_2O)$, i.e., electrostatic plus dispersion, repulsion, and cavitation) free energy of solvation have been also considered on a number of complexes. To this aim, they have been embedded in aqueous solution employing the integral equation formalism for the polarizable continuum model (IEF-PCM),[21] allowing their structures to relax. The MIA in solution was evaluated in analogy with eq 5, associating the full cavity to each partner, kept rigid in the geometry optimized in solution for that complex. Natural bond orbital (NBO)[22] and natural population analyses (NPA)[23] were also carried out to clarify the nature of the bonding. Extensive comparisons with the copper binding/chelating ability of plicatin B have been carried out in an attempt to correlate it with their experimental potency as antioxidants.[13]

III. Results and Discussion

The structures of the bitucarpin A and erybraedin C isolated pterocarpans (schemes, atom numbering, and torsional degrees of freedom in Chart 1) have been investigated in a previous study,[11] where full details can be found. However, in order to make this article self-contained, a few definitions are reported

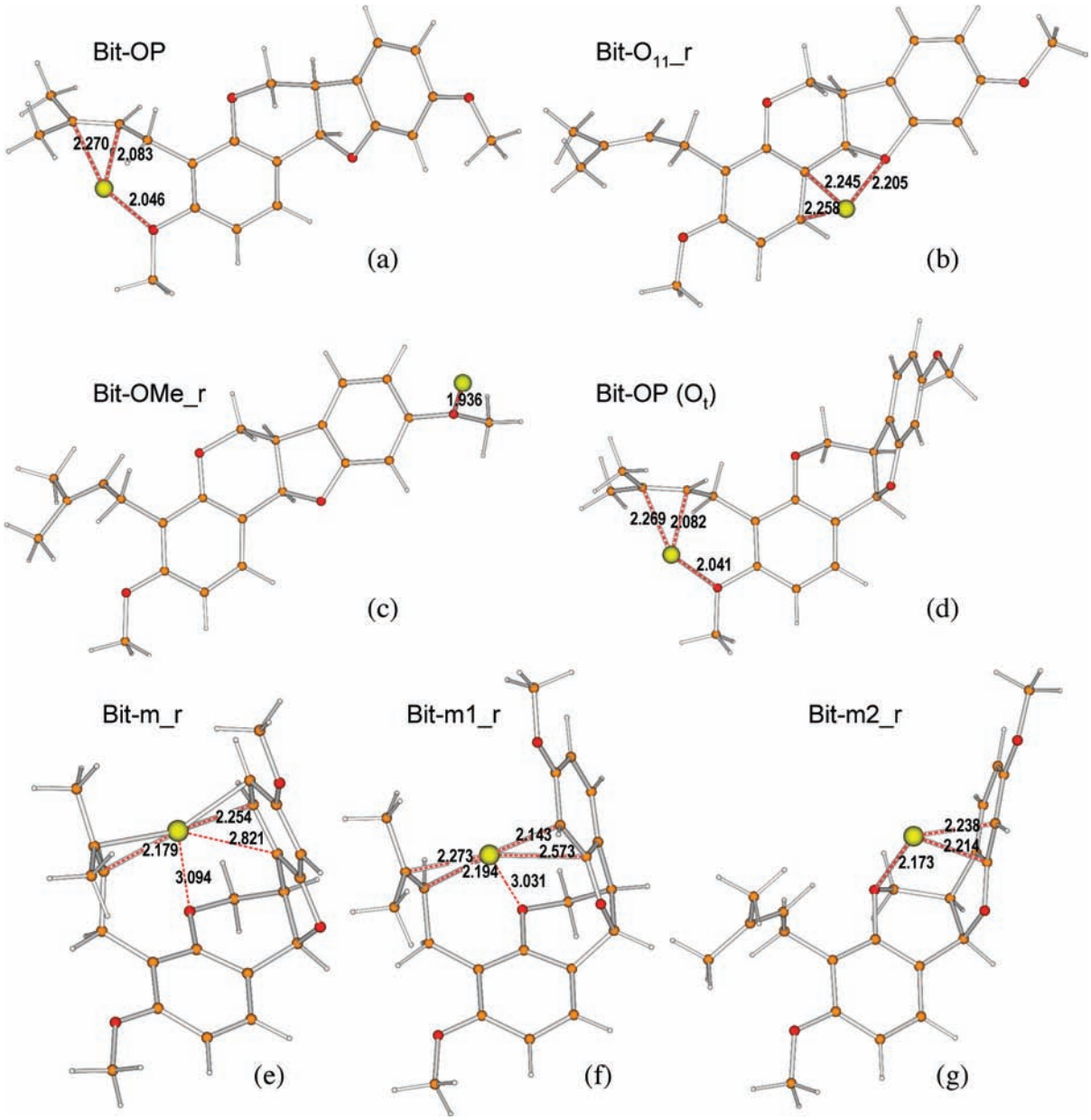

Figure 1. B3LYP/6-31G* structures (drawn with Molden: Schaftenaar, G.; Noordik, J. H. *J. Comput.-Aided Mol. Des.* **2000**, *14*, 123−134; distances in Å) of low-energy $Cu^{2+}\cdots$bitucarpin A complexes: (a−c) H_t arrangement; (d−g) O_t arrangement.

hereafter. The cis structure refers to the (6a*R*,11a*R*) diastereomer in this case, with O_{11} pseudoaxially oriented to avoid steric interaction with the *peri* C_1 hydrogen. With the other cis diastereomer, its mirror image (6a*S*,11a*S*), constitutes the natural occurring form, whereas the trans diastereomers, i.e., (6a*R*,11a*S*) and (6a*S*,11a*R*), not considered herein, are significantly strained and turn out to be less stable than the cis ones by ∼10 kcal/mol.[11] In addition for both pterocarpans, the cis fused ring backbone exhibits two different arrangements, named H_t and O_t depending on which atom at position 6 is trans with respect to H_{6a}. At the B3LYP/6-31G* level, the H_t structure is ∼2 kcal/mol more favorable than the O_t one, regardless of the nature and number of substituent groups. The pterocarpan skeleton constitutes a two-blade system with considerably different values of the angles between the blades in H_t (∼145°) and O_t (∼100°). The interconversion between the H_t and O_t structures occurs with barrier heights of about 6−7 kcal/mol along two pathways. The remarkable flexibility of the fused ring system is due to the presence of a CH_2 group in one of the rings and to the capability of the $C_1C_{1a}C_{11a}O_{11}$ dihedral angle to distort itself although belonging to a ring. After recollecting these basic concepts and results, the binding sites of Cu^{2+} on both flexible ligands with their relevant affinities in vacuo and in solution are discussed.

A. Preferred Binding Sites of Copper(II) Cations in Vacuo. A number of complexes to illustrate the preferred binding sites of Cu^{2+} on bitucarpin A and erybraedin C are displayed in Figures 1 and 2, with their affinity values and deformation effects reported in Tables 2 and 3, respectively. In the figures and tables, reference is made to the Cu(II) binding sites involving prenyl groups and/or the hydroxy/methoxy region (OP, OH/OMe complexes); when the group at C_9 (or even C_3 for erybraedin) is rotated, the suffix "_r" is appended to the complex name. (For bitucarpin A, _r corresponds to $C_{10}C_9OMe$ in transoid position; for erybraedin C, _r corresponds to C_2C_3OH or $C_{10}C_9OH$ in cisoid position (refer to the figures in the Supporting Information for clarity).) In contrast, when Cu^{2+} is bridged between the two blades, in other words the coordination

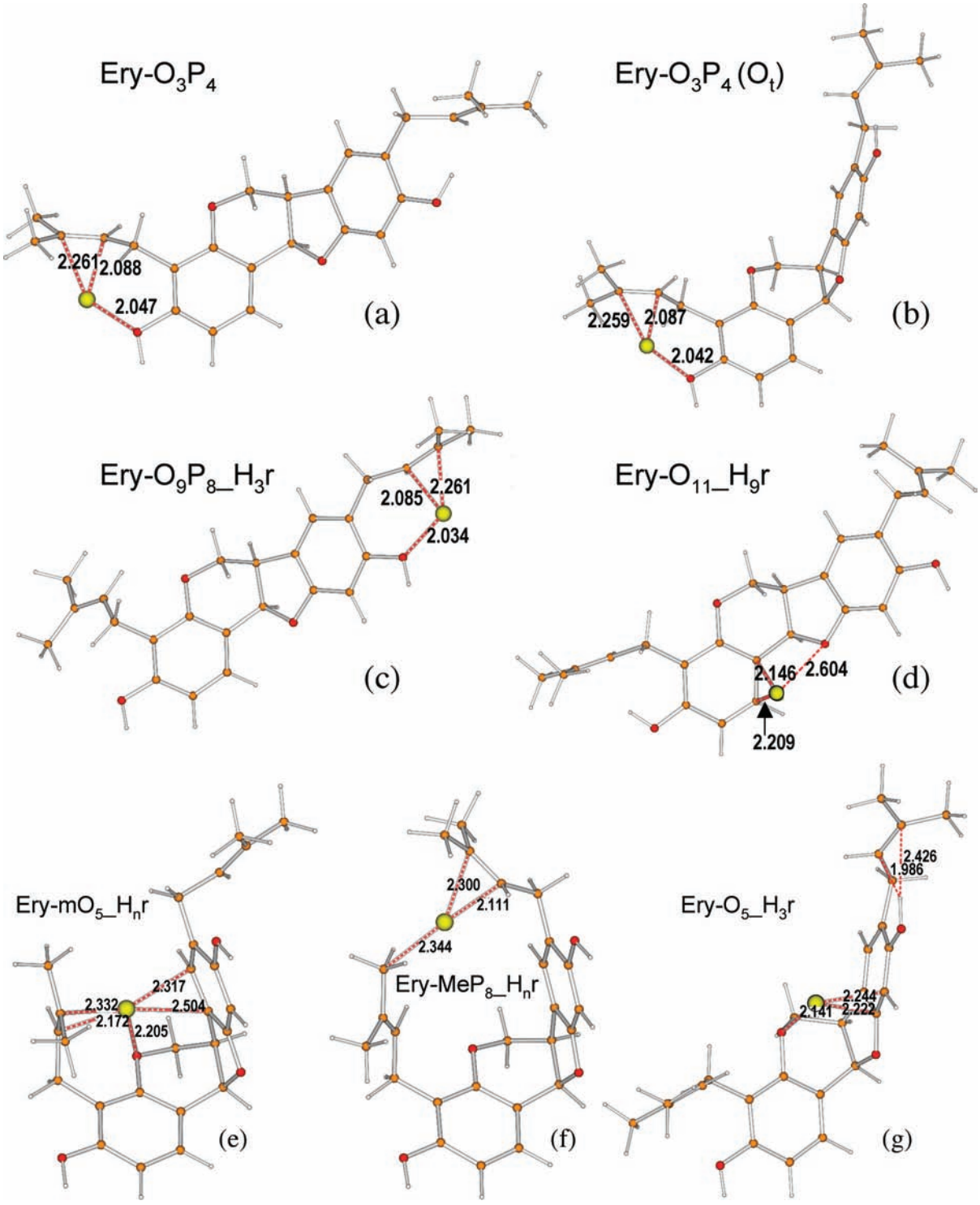

Figure 2. B3LYP/6-31G* structures of low-energy $Cu^{2+}\cdots$erybraedin C complexes: (a) H_t arrangement; (b) O_t arrangement; (c, d) H_t arrangement; (e−g) O_t arrangement.

involves ligand groups on both sides of the pterocarpan, the complex name contains an "m", standing for "mixed", and an Arabic number, if necessary, to avoid mentioning all groups involved in the binding interactions that would produce tricky strings of characters. Therefore, especially for these adducts, it is advisable to refer to the figures (the full set can be found in the Supporting Information (pp 16−26)). In order to clarify matters, the starting arrangement for a few structures is described, because the preferential trends along the minimization paths permit to exclude the occurrence of particular complexes that in principle might be considered stable.

1. Bitucarpin A. According to the schematic representation of bitucarpin A, displayed in Chart 1, a number of coordination sites for Cu^{2+} can be identified, which include the ethereal O regions of the rings and of the methoxy side chains, besides the aromatic ring and prenyl π densities. For the H_t arrangement of the pterocarpan, starting from structures with Cu^{2+} bridged between O_5 and the adjacent aromatic bond (involving or not the prenyl double bond), an OP arrangement (**Bit-OP**, Figure 1a) is invariably obtained, which corresponds to the most stable complex ($-1349.268374E_h$) with a very favorable MIA (370.3 kcal/mol) and $E_{def} = 11.9$ kcal/mol (see Table 2).

TABLE 2: B3LYP/6-31G* Metal Ion Affinities (MIA) and Cu^{2+} Separations of Low-Energy $Cu^{2+}\cdots$Bitucarpin A Complexes[a]

	complexes	MIA	E_{def}	$Cu^{2+}\cdots C$	$Cu^{2+}\cdots OMe/O_{11}/O_5$	$Cu^{2+}\cdots C$
1a	**Bit-OP**	370.30[b]	11.90	2.083	2.046	2.270
	Bit-OP_r	367.88	11.84	2.084	2.045	2.271
1b	**Bit-O_{11}_r**	337.54	7.31	2.258	2.205	2.245
	Bit-O_{11}	336.98	7.21	2.286	2.244	2.199
	Bit-OMe	341.70	12.02		1.962	
1c	**Bit-OMe_r**	343.61	13.95		1.936	
1d	**Bit-OP (O_t)**	371.06	12.41	2.082	2.041	2.269
	Bit-m	362.70	16.99	2.175		2.211
1e	**Bit-m_r**	365.38	21.03	2.179		2.254
1f	**Bit-m1_r**	370.86	25.13	2.194		2.143
	Bit-m1	368.55	24.39	2.194		2.160
1g	**Bit-m2_r**	343.17	14.72	2.214	2.173	2.238
	Bit-m2	340.76	13.81	2.211	2.165	2.264

[a] Separations in angstroms, MIA and E_{def} in kcal/mol. [b] Cu^{2+} reference energy $= -195.065696E_h$.

By rotating the methoxy group at C_9 about the C_9-OMe bond (φ_1), the second most stable H_t complex (**Bit-OP_r**) is reached that features analogous separations between Cu^{2+} and chelating groups as **Bit-OP**. Although the mutual position of the partners does not appreciably change, the MIA somewhat decreases, becoming 367.9 kcal/mol, with E_{def} equal to 11.8 kcal/mol.

It is worth recalling that the B3LYP MIA turned out to be substantially higher (by ~20−30 kcal/mol) than that obtained using the Becke's half-and-half (BH)[24] nonlocal hybrid exchange functional coupled to the LYP correlation functional (BHLYP) in our recent study on plicatin B.[12] This confirmed the propensity of the B3LYP functional to overestimate the binding energies when Cu^{2+} is involved, while calculations with BHLYP (in which the exact exchange mixing is 50%) were reported to provide very good agreement with CCSD(T) for ground and low-lying states of $Cu^{2+}-H_2O$.[25] However, the conserved trend for the lines correlating B3LYP to BHLYP MIA and ΔE values ($r = 0.980$ and 0.974, respectively) indicated that the MIA values, although overestimated, were fairly comparable among them as well as the relative stabilities of the complexes and thus suitable to be used for comparative purposes.

The least favorable coordination sites among those reported in Table 2 concerning the MIA correspond to the O_{11} region (i.e., **Bit-O_{11}_r,** displayed in Figure 1b, and **Bit-O_{11}**) with a very limited effect due to the methoxy group rotation. They are less stable than **Bit-OP** by about 28.5 kcal/mol; moreover, relaxing their geometries once Cu^{2+} has been removed the closest minima lie ~7 kcal/mol below. (Since the geometry deformation is very limited, this value can be attributed to the relaxation of the electronic distribution (the ligand in the complex has an unpaired electron, as stated below).) Those coordination structures are also obtained starting from tentative arrangements with Cu^{2+} located above the six-membered heteroring (B in Chart 1). The MIA of the complexes with Cu^{2+} coordinated to the methoxy oxygen at C_9, i.e., **Bit-OMe** and **Bit-OMe_r** (the latter displayed in Figure 1c), are somewhat larger than 340 kcal/mol. Their stabilities are however similar to the **Bit-O_{11}** ones.

Conversely the scaffold structures remarkably change going from H_t to O_t arrangements, because of the value assumed by the dihedral angle between the two blades of the pterocarpan fused ring system, reported above. The O_t arrangement allows another stable Bit-OP structure to be located, named **Bit-OP (O_t)** (Figure 1d), which turns out to be the second most stable complex, higher in energy than **Bit-OP** by just 1.76 kcal/mol, due to the ring strain in the O_t structure. Interestingly enough, the most favorable MIA is obtained for this complex showing limited deformation energy (12.4 kcal/mol). The short separation of the C and D rings from O_5 and the prenyl side chain allows the metal ion to be sequestered inside a variety of groups (the π density of prenyl groups and aromatic rings as well as the O_5 lone pairs). When Cu^{2+} interacts with both chelating arms (Figure 1, parts e and f), the MIA is on the average very favorable ranging from 362.7 to 370.9 kcal/mol (a value very close to that corresponding to **Bit-OP (O_t)**). Those arrangements however are obtained at the expense of some strain energy penalty. Actually, after the removal of Cu^{2+} the strain energy is released ($17 \le E_{def} \le 25.1$ kcal/mol). Adducts involving O_5 and just one of the chelating arms are also obtained, such as **Bit-m2_r** (Figure 1g) and **Bit-m2**.

2. Thermal and Counterpoise Corrections on Bitucarpin A Complexes with Cu^{2+}. Thermal and counterpoise corrections have been investigated for the complexes of bitucarpin with copper(II), because one of the referees was concerned about entropic effects on the relative stability and the other raised some doubts about the possible incidence of basis set superposition errors on metal ion affinities for a basis set of limited size. The results obtained for the 13 complexes in Table 2 are reported in Table 3. In order to distinguish relative stabilities from metal ion affinities, for the latter values only in this section the symbols MIA(E), MIA(H_{298}), and MIA(G_{298}) have been used.

As expected, the entropic effect is lower (~−52 kcal/mol) for polydentate structures, where the ion is chelated between two end groups, such as in the **Bit-m**, **Bit-m1**, and **Bit-OP** complexes. The entropic effect is intermediate (~−54 kcal/mol) for the **Bit-m2** complexes, where the ion is dentated between a ring heteroatom and one of the end groups, while it is the highest (~−55 kcal/mol), but still within 3 kcal/mol of the lowest values, when the ion is coordinated to a double bond (hapticity = 2) as in **Bit-O_{11}** or when it is monodentate as in **Bit-OMe**. Interestingly enough, energy, enthalpy, and free energy based values behave in an analogous way: no inversion in the relative stabilities or in the metal ion affinities is observed in this series of complexes, supporting our choice, tested for plicatin B, of using energy based values.

The counterpoise corrected interaction energy, which taken as the negative can be considered a counterpoise corrected MIA, parallels the MIA(E). It is slightly less favorable (by ~0.8−1.5%), because the BSSE ranges from 2.7 to 5.6 kcal/mol. Therefore, while counterpoise corrections can be important for H-bonding interactions with neutral molecules, such as water,[26] they appear to be almost uninfluent for large interaction energies, especially for comparative purposes as in the present case.

Of course, we do not claim to have considered all the possible adducts, but at least a representative set of them. We are confident that no Cu^{2+} complex at O_5 is stable with the H_t scaffold arrangement, because the metal ion migrates toward the electron-rich methoxy O-prenyl (OP) region. No coordination sites are located right above or below the pterocarpan blades either, because Cu^{2+} prefers to bind above the outer region in the vicinity of O_{11}, C_{1a}, and C_1, although the MIA is the lowest determined in this study. The MIA on lone pairs of the methoxy O at C_9 is just somewhat more favorable. When the O_t fused-ring structure is considered, chelated arrangements are obtained with high MIA. If the prenyl group is not involved in the interaction, the MIA is reduced to the same value calculated at the methoxy O at C_9 for H_t.

The list including labels, structures, absolute energies of the complex ([Ligand$\cdots Cu^{2+}]_{(i)}$), of the ligand in the complex (Ligand$_{(i)}$), of the ligand optimized structure related to that

TABLE 3: B3LYP/6-31G* Relative Stabilities and Metal Ion Affinities in Terms of Energy, Enthalpy, and Free Energy[a]

		relative stability			metal ion affinity				
	complexes	ΔE	ΔH_{298}	ΔG_{298}	(E)	(H_{298})	(G_{298})	ΔE^{CP}	BSSE
1a	**Bit-OP**	0[b]	0[c]	0[d]	370.29	369.18	371.52	−366.02	4.27
	Bit-OP_r	2.55	2.43	2.14	367.88	366.74	369.48	−363.64	4.24
1b	**Bit-O_{11}_r**	28.35	27.42	24.53	337.54	337.32	342.62	−333.38	4.16
	Bit-O_{11}	28.69	27.78	24.97	336.98	336.72	341.82	−332.35	4.63
	Bit-OMe	28.73	28.36	25.13	341.70	340.96	346.52	−338.96	2.74
1c	**Bit-OMe_r**	28.77	28.42	25.32	343.61	342.82	348.22	−340.75	2.87
1d	**Bit-OP (O_t)**	1.76	1.78	1.64	371.06	369.83	371.80	−366.39	4.67
	Bit-m	14.67	14.00	14.65	362.70	362.18	363.48	−357.20	5.50
1e	**Bit-m_r**	16.22	15.66	15.64	365.38	364.76	366.76	−360.00	5.38
1f	**Bit-m1_r**	14.88	14.41	14.96	370.86	370.08	371.05	−365.26	5.60
	Bit-m1	16.24	15.76	16.42	368.55	367.81	368.96	−363.01	5.54
1g	**Bit-m2_r**	32.11	31.18	29.76	343.17	342.90	345.97	−338.27	4.89
	Bit-m2	33.45	32.45	31.12	340.76	340.56	343.75	−335.88	4.88

[a] The counterpoise corrected interaction energies (ΔE^{CP}) are also reported together with the basis set superposition errors (BSSE) for low-energy $Cu^{2+}\cdots$bitucarpin A complexes. Units in kcal/mol. [b] $-1349.268374E_h$. [c] $-1348.822686E_h$. [d] $-1348.905890E_h$.

TABLE 4: B3LYP/6-31G* Metal Ion Affinities (MIA) and Cu^{2+} Separations of Some Low-Energy $Cu^{2+}\cdots$Erybraedin C Complexes[a]

	complexes[b]	MIA	E_{def}	$Cu^{2+}\cdots C$	$Cu^{2+}\cdots OH/O_5/O_{11}$	$Cu^{2+}\cdots C$
2a	**Ery-O_3P_4**	376.54	11.62	2.088	2.047	2.261
2b	**Ery-O_3P_4(O_t)**	377.43	12.51	2.087	2.042	2.259
	Ery-O_3P_4_H_9Pr (O_t)	379.58	13.61	2.087	2.035	2.255
	Ery-O_3P_4_H_9r (O_t)	378.88	12.88	2.087	2.042	2.259
2c	**Ery-O_9P_8_H_3r**	377.03	14.64	2.085	2.034	2.261
2d	**Ery-O_{11}_H_9r**	350.39	11.53	2.209	2.604	2.146
	Ery-O_{11}	344.98	9.89	2.174	2.678	2.171
	Ery-O_{11}_H_3r	342.29	6.98	2.244	2.224	2.249
2e	**Ery-mO_5_H_nr**	373.29	18.18	2.172	2.205	2.317
	Ery-mO_5_H_nPr	368.69	16.92	2.182	2.203	2.318
	Ery-mO_5_H_3r	365.00	15.90	2.182	2.198	2.305
	Ery-mP_4_H_nr	371.97	22.62	2.191	2.811	2.211
2f	**Ery-MeP_8_H_nr**	359.18	12.96	2.344		2.111
2g	**Ery-O_5_H_3r**	347.42	14.99	2.211	2.141	2.222

[a] Separations in Å, MIA and E_{def} in kcal/mol. [b] Hydrogens are named after the O they are bonded to.

complex (Ligand$_{(i,opt)}$), E_{def} and MIA is reported in Table S1 of the Supporting Information.

3. Erybraedin C. The presence of an additional prenyl group (at C_8) and of hydroxy moieties in place of methoxy ones does not substantially alter the coordination behavior of the ligand, as can be inferred from the results reported in Table 4 and in Figure 2. Due to the presence of two hydroxy groups adjacent to the prenyl side chains, the structures are named with the _H_nr suffix when both phenolic hydrogens are rotated in opposite direction with respect to the prenyl side chains (or with the _H_nPr suffix when also the P_8 prenyl group is rotated about φ_5). This obviously prevents intramolecular H-bond formation with the double bond π density. The absence of the _H_nr suffix, however, does not mean per se the occurrence of the aforementioned H bonds, because of the prenyl group remarkable flexibility. Conversely, when just one of the phenolic hydrogens is rotated, n takes the value 3 or 9, depending on the case, with the usual warning about H bonds. Thus the structure names do not account for H bonds. It is necessary to refer to the figures to check if H bonds are present (all structures with the relevant discussion can be found on pp 19−26 of the Supporting Information). As a general rule, H bonds slightly affect the stability of the system but not its metal ion affinity. Probably they would be much more important for other kinds of mechanisms of activity,[13,27] such as those involving hydrogen atom donation, but not for that here considered, that is the protection against copper-mediated oxidative damage, that may involve both a sequestering and a reducing action of the ligands. Interestingly enough, experimental data[28] have suggested that prenylchalcones and α,β-unsaturated keto functionality (compounds belonging to the same class as plicatin B) provide protection against oxidative modification of LDL and are more potent inhibitors than their nonprenylated analogues. Actually, in section D the capabilities of these moieties will be briefly discussed.

A number of additional structures can be found with the label cell highlighted in yellow in Table S2 of the Supporting Information, inserted after those selected for detailed discussion. The latter ones have been reported in order of descending stability within each class of complexes. The list contains labels, structures, absolute energies of each complex, of erybraedin C in that complex (Ligand$_{(i)}$), of the erybraedin C optimized structure related to that complex (Ligand$_{(i,opt)}$), E_{def}, the metal ion affinity (MIA), and the relative stability with respect to the coordination complex taken as zero.

Similarly to that found for bitucarpin A when the geometry optimization started from structures with Cu^{2+} bridged between O_5 and the adjacent aromatic bond (involving or not the prenyl double bond), for the H_t scaffold structure an O_3P_4 arrangement of the metal ion has been located (**Ery-O_3P_4**, Figure 2a), with Cu^{2+} placed between the O_3 lone pairs and the P_4 double bond π density. This is the most stable coordination complex here obtained ($-1466.010426E_h$). Its MIA is very favorable as well (376.5 kcal/mol, see Table 4), although it does not correspond to the best value.

On examination of Figure 2a, it is evident that H_9 is H bonded to the P_8 double bond π density (C_9C_8CC and $C_8CCC = -45.0°$ and 133.1°, respectively). Considering the O_t scaffold arrangement, an analogous coordination complex (**Ery-$O_3P_4(O_t)$**, Figure 2b), albeit less stable than the H_t one by 1.98 kcal/mol due to the scaffold strain, is found. Conversely, its MIA is somewhat more favorable (377.4 kcal/mol), while the $H_9\cdots P_8$ H bond is conserved. Since the affinity to the metal is stronger in the O_t scaffold arrangement, additional structures of this type have been considered. A very similar stability, deformation energy, and MIA are obtained when the P_8 prenyl side chain is rotated by ~90° about φ_5 and its double bond is still engaged in the H bond with the phenolic OH ($C_9C_8CC = 45.2°$, see Table S2 of the Supporting Information).

When the polar H at O_9 points to the prenyl side chain, but the H bond is prevented due to the adverse prenyl group dihedral values, the MIA for this local minimum decreases only slightly, becoming 376.0 kcal/mol. Rotating the phenolic OH at C_9 and starting with Cu^{2+} bridged above O_5 and C_{4a}, the fourth most stable complex among those reported in Table 4 (**Ery-O_3P_4_H$_9$Pr (O_t)**) is reached, with separations between Cu^{2+} and the chelating groups analogous to **Ery-$O_3P_4(O_t)$**. In this orientation of the phenolic OH, no H-bond is feasible and the prenyl double bond at P_8 rotates farther from the O lone pairs. The MIA, however, turns out to be 379.6 kcal/mol, the best obtained for this compound. **Ery-O_3P_4_H_9r (O_t)** is the third most stable complex in Table 2, with MIA = 378.9 kcal/mol, even though a different orientation of the prenyl moiety prevents H-bonding at P_8.

When considering the attack onto the O_9P_8 end of H_t erybraedin C, with the O_3H group rotated (**Ery-O_9P_8_H_3r**, Figure 2c), the stability and the MIA (377.0 kcal/mol) are slightly less favorable than those obtained on the other terminus. Since the mutual position of the partners does not appreciably change, the difference is mainly due to the presence of a five-membered heteroring in place of a six-membered one. On this blade of the molecule, the rotation of the P_8 prenyl side chain about φ_5 was taken into account. This fact produced somewhat longer separations (by about 0.01−0.02 Å) between metal ion and ligand groups with a decrease in the MIA by 1 kcal/mol.

The MIA of the subsequent structures with the H_t scaffold arrangement is less favorable by about 27−30 kcal/mol than that of those discussed thus far. All the complexes with Cu^{2+} coordinated in the O_{11} region (this definition is just to expedite matters; actually the $O_{11}\cdots Cu^{2+}$ separation can be longer than that of $C_{1a}\cdots Cu^{2+}$) derive from starting geometries with the metal cation located above the six-membered heteroring, although not displaced enough to resent the attraction of the electron-rich tails. **Ery-O_{11}_H_9r**, shown in Figure 2d, features the metal cation bridged above C_1 and C_{1a} (MIA = 350.4 kcal/mol), with H_3 H-bonded to P_4, while H_9 is rotated outward. When both tails are H-bonded, as in **Ery-O_{11}**, the separation of Cu^{2+} from C_{1a} and O_{11} is somewhat longer, making the MIA decrease by nearly 5 kcal/mol. A similar effect is found for **Ery-O_{11}_H_nr**, i.e., when no H-bond is present in the tails. Conversely, with H_3 H-bonded to P_4 and H_9 rotated inward, but not involved in an H-bond with P_8, the MIA is 346.5 kcal/mol.

For **Ery-O_{11}_H_3r** (H-bond in the H_9-P_8 tail), the shortest distance is $O_{11}\cdots Cu^{2+}$, while $C_1\cdots Cu^{2+} \approx C_{1a}\cdots Cu^{2+}$ are only slightly longer (MIA = 342.3 kcal/mol). An analogous behavior is found in the case of **Ery-O_{11}_H_3r** without the H-bond in the H_9-P_8 tail.

TABLE 5: B3LYP/6-31G* NPA Charges (*e*) and Spin Density on the Metal Ion in a Number of Complexes in Vacuo for Bitucarpin A and Erybraedin C

structures	NPA	spin density	structures	NPA	spin density
Bit-OMe	0.9039	−0.0000	**Ery-O_3P_4**	0.8647	−0.0000
Bit-OP	0.8652	−0.0000	**Ery-$O_3P_4(O_t)$**	0.8665	0.0000
Bit-O_{11}	0.8801	0.0004	**Ery-O_{11}_H_9r**	0.8602	−0.0002
Bit-m	0.8928	0.0258	**Ery-O_9P_8_H_3r**	0.8628	0.0000
Bit-m1_r	0.8124	−0.0005	**Ery-mO_5_H_nPr**	0.9021	0.0299
Bit-m2_r	0.8783	0.0035			
Bit-O_{11}_r	0.8864	0.0004			

Concerning the other structures with the O_t backbone arrangement, the smaller value of the dihedral angle between the scaffold blades allows chelation of Cu^{2+}. The most favorable complexes are obtained when the metal cation is chelated between the D ring and the facing P_4 double bond, as in the structures displayed in Figure 2e. In **Ery-mO_5_H_nr** (MIA = 373.3 kcal/mol) the closest contacts between Cu^{2+} and erybraedin involve O_5 and one of the double bond C of P_4. The distance from the other double bond C of P_4 is only slightly longer than that from C_7. Another local minimum, **Ery-mO_5_H_nPr** (MIA = 368.7 kcal/mol) is found for P_8 rotated by ~120° about φ_5 with all the other features of the complex practically unaltered. The scaffold and chelating arrangements are maintained also in **Ery-mO_5_H_3r** (MIA = 365.0 kcal/mol) that conversely exhibits an H-bond between H_9 and the P_8 π density. **Ery-mP_4_H_nr**, the last complex of this type considered (MIA = 372.0 kcal/mol), without H-bonds, has been obtained starting with the metal cation located above C_1. However, although smaller than for H_t, the dihedral angle between the blades is still large. Therefore, chelation, i.e., coordination involving both prenyl double bonds in this case, is prevented. In order to check this result, a number of constrained optimizations have been performed first. After the geometries are relaxed, the only favorable arrangement found, **Ery-MeP_8_H_nr** (Figure 2f, with MIA = 359.2 kcal/mol), where the closest contacts involved both double bond C of P_8 and the C of the nearby methyl group of P_4. In the final class of complexes, Cu^{2+} is bridged between O_5 and C_{10a}, with a significant interaction with C_{10} as well. **Ery-O_5_H_3r** (Figure 2g, MIA = 347.4 kcal/mol) is displayed as a representative complex with an H bond in the H_9P_8 tail. In the absence of H bonds the MIA decreases, becoming 350.0 or 343.7 kcal/mol, depending on the rotation of the prenyl side chain.

In analogy to bitucarpin A, the counterpoise corrected metal ion affinity is less favorable by <1%, because the BSSE ranges from 3.9 to 5.6 kcal/mol.

B. Copper Charges and Analysis of the Bonding. The ion charge in the free state is obviously +2 for Cu^{2+}. Conversely, the NPA charges on the metal ion, reported in Table 5 for few different complexes of the two ligands here considered, show values remarkably lower than 2. All of them are close to 0.9*e* and do not show appreciable dependence on the system and on the coordination complex structure. They actually range from 0.81 (**Bit-m1_r**) to 0.90*e* (**Bit-OMe**) for bitucarpin A and from 0.86 (**Ery-O_{11}_H_9r**) to 0.90*e* (**Ery-mO_5_H_nPr**) for erybraedin C, respectively.

According to this fact, the spin density on the copper ion testifies that the dication in the complex is reduced by the ligand, becoming Cu^+, with d^{10} electronic configuration (Table 6). The ligand turns out to be a positively charged radical, with the charge distributed farther apart from the metal ion and primarily on the originally (i.e., in the isolated ligand) electron-rich C atoms belonging to the prenyl moieties or to the fused ring

TABLE 6: B3LYP/6-31G* Natural Atomic Orbital Occupancies of Some Valence Orbitals in the Isolated Metal Ion and in a Number of Complexes with Bitucarpin A (top) and Erybraedin C (bottom)

orbitals	Cu^{2+}	**Bit-OMe**	**Bit-OP**	**Bit-O_{11}**	**Bit-m**	**Bit-m1_r**	**Bit-m2_r**	**Bit- O_{11}_r**
s (4s)	0.00002	0.12683	0.23621	0.15810	0.25194	0.31930	0.18754	0.15092
d_{xy} (3d)	1.99993	1.96906	1.98820	1.99119	1.99703	1.97949	1.98900	1.97617
d_{xz} (3d)	1.99991	1.99453	1.94087	1.98689	1.98111	1.99686	1.98111	1.99565
d_{yz} (3d)	1.99993	1.99462	1.99448	1.97580	1.94439	1.94858	1.98243	1.98814
$d_{x^2-y^2}$ (3d)	1.74975	1.99780	1.96964	1.99020	1.97971	1.94874	1.98261	1.98628
d_{z^2} (3d)	1.24965	1.99157	1.99097	1.99347	1.93828	1.98416	1.97406	1.99237

orbitals	Cu^{2+}	**Ery-O_3P_4**	**Ery-$O_3P_4(O_t)$**	**Ery-O_{11}_H_9r**	**Ery-O_9P_8_H_3r**	**Ery-mO_5_H_nPr**
s (4s)	0.00002	0.23555	0.23474	0.18386	0.23964	0.23625
d_{xy} (3d)	1.99993	1.98095	1.98394	1.99475	1.98647	1.95780
d_{xz} (3d)	1.99991	1.95781	1.95870	1.99772	1.97116	1.98632
d_{yz} (3d)	1.99993	1.99402	1.99479	1.96439	1.99616	1.95994
$d_{x^2-y^2}$ (3d)	1.74975	1.97830	1.97435	1.97855	1.96783	1.96028
d_{z^2} (3d)	1.24965	1.97389	1.97219	1.99474	1.96083	1.97976

double bonds. A small fraction of the spin density can be found also on the O atom located farther apart from the metal ion. This result had been reported earlier for uracil.[29] Interestingly, in erybraedin both phenolic hydrogens show a significantly positive NPA charge (0.52*e*).

Therefore, the main effect observed upon formation of the complexes is the variation in the occupancies of the 4s and 3d orbitals, as can be inferred from a perusal of Table 6. The trend is similar for the Cu^{2+} complexes of both ligands.

Since an analysis of the electronic distribution can be helpful in suggesting suitable modifications and/or appropriate substituents to enhance the stability of the coordination complexes with Cu^{2+}, a detailed discussion of a few typical complexes is provided in the Supporting Information (pp 70−73). The donor−acceptor interactions can be determined from the second-order perturbation theory analysis of the Fock matrix in the NBO basis. Of course the donor orbitals involved are different depending on the coordination site involved. Useful pieces of information can be derived from that analysis: interested readers are referred to it.

C. Preferred Binding Sites of Copper(II) Cations in Aqueous Solution. Since the interactions here considered occur in aqueous solution, the solvent effect has been taken into account in the framework of the polarizable continuum model. The effect of explicit water molecules had been considered earlier for these ligands, using as starting arrangements for the optimizations cluster structures derived from molecular dynamics simulations,[30] but the results confirmed the importance of specific H-bonding interactions without affecting the stability order.[26] In any case, the competition between metal ion and ligand can be satisfactorily addressed with PCM, because water is expected to bind preferentially to the metal cation (whose charge is much more localized than that on the ligand); thus its primary effect is the screening of the metal ion charge. The effect of explicit water molecules was examined for bitucarpin and erybraedin,[26] to allow determination of their preferential hydration sites. (The importance of the dipole moment orientation in neutral molecules was also discussed, because the solvent reaction field is stronger when dominated by a dipolar component than by a quadrupolar one.) Of course, the early stages of the ligand−dication interaction should significantly change when including specific solvation effects (partial desolvation at least should occur), although for Cu^{2+} the reaction can still be easily produced.[31] This interesting investigation is however beyond the scope of the present study, aimed at comparing the behavior of the complexes with Cu^{2+} of bitucarpin and erybraedin to that of plicatin B, already examined[12] in a continuum solvent (water) using IEF-PCM, and will be postponed to a forthcoming article.

TABLE 7: IEF-PCM/B3LYP/6-31G* Metal Ion Affinities (MIA), $E_{def}(w)$, G_{sol}, G_{sol}(def), ΔG_{tot} (kcal/mol) of Low-Energy $Cu^{2+}\cdots$Bitucarpin A Complexes in Aqueous Solution[a]

complexes	MIA	E_{def}(w)	G_{sol}	G_{sol}(def)	ΔG_{tot}
Bit-OP	263.70	0.67	−109.83	−109.16	0[b]
Bit-OP (O_t)	264.27	1.02	−111.27	−110.25	0.67
Bit-O_{11}_r	207.90	3.73	−124.16	−120.43	17.07
Bit-O_{11}	210.42	3.16	−126.24	−123.07	14.77
Bit-OMe	183.48	0.99	−115.21	−114.22	23.67
Bit-m	327.03	2.59	−119.28	−116.69	7.14
Bit-m1_r	326.99	1.63	−115.15	−113.52	10.52
Bit-m2_r	229.21	2.80	−120.21	−117.41	23.87

[a] See text. [b] Reference $G_{tot} = -1349.442328E_h$.

We briefly recollect the meaning of the physicochemical magnitudes mentioned in what follows: G_{sol}(def) is the total solvent effect (accounting also for the deformation due to the solvent field) that can be derived from the separation between the total free energy in solution, named $G(H_2O)$, and ΔE(vac). The impact of the aqueous solvent in the IEF-PCM framework, using the UA0 radii as in ref 12, has been also considered for a number of representative coordination complexes of both pterocarpans, because in the previous study on plicatin B the gas phase high energy complexes turned out to be remarkably stabilized in solution, while the MIA was reduced because of the competition between the solvent reaction field and the ligand.[12] The binding sites of Cu^{2+} on bitucarpin A and erybraedin C do not change appreciably going from the gas phase to the continuum aqueous solution, as can be inferred also from the values of $E_{def}(w)$, that do not affect too much the always stabilizing solvent effect, very high due to the presence in solution of a net charge (+2), distributed on the coordination complexes as described above, that produces a strong electrostatic field. Therefore it is advisable to refer to the corresponding structures in vacuo, without showing hardly distinguishable structures in solution, whereas the affinity values in solution are reported in Tables 7 and 8, respectively, together with other quantities of interest.

1. Bitucarpin A. The relative potential energies in vacuo and the relative free energies in solution ($\Delta G(H_2O)$) are displayed in Figure 3 for a number of complexes of bitucarpin A with Cu^{2+}.

A visual estimate of the total solvent effect for each complex can be derived from the separation between the line corresponding to the potential energy in vacuo and that of the total free energy in aqueous solution. As observed earlier, the solvent effect dampens the free energy differences, especially when the ion is remarkably exposed to the solvent.

TABLE 8: IEF/PCM/B3LYP/6-31G* Metal Ion Affinities (MIA), $E_{def}(w)$, G_{sol}, $G_{sol}(def)$, ΔG_{tot} (kcal/mol) of Low-Energy $Cu^{2+}\cdots$Erybraedin C Complexes in Aqueous Solution[a]

complexes[b]	MIA	E_{def}(w)	G_{sol}	G_{sol}(def)	ΔG_{tot}
Ery-O$_3$P$_4$	258.84	1.32	−114.81	−113.49	0[b]
Ery-O$_3$P$_4$(O$_t$)	261.71	1.65	−116.28	−114.62	0.85
Ery-O$_9$P$_8$_H$_3$r	260.64	1.83	−116.37	−114.54	3.70
Ery-O$_{11}$_H$_9$r	221.97	2.61	−126.11	−123.50	16.19
Ery-mO$_5$_H$_n$r	347.28	2.58	−126.88	−124.30	3.19
Ery-mO$_5$_H$_n$Pr	360.21	3.08	−126.46	−123.38	7.34
Ery-O$_5$_H$_3$r	241.08	2.84	−125.28	−122.44	25.52

[a] See text. [b] Reference $G_{tot} = -1466.191281 E_h$.

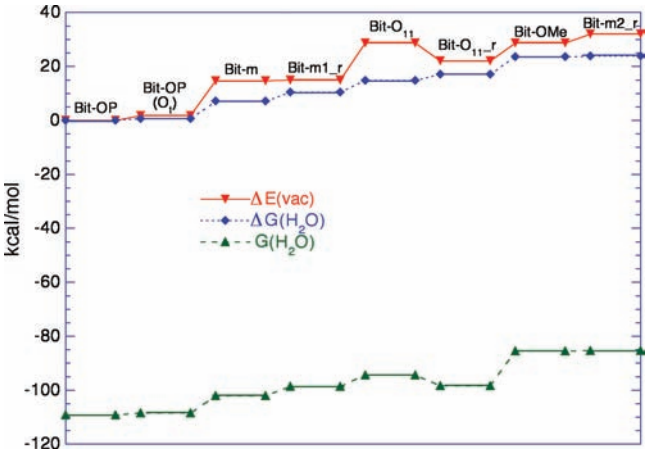

Figure 3. IEF-PCM/B3LYP/6-31G* relative free energies ($\Delta G(H_2O)$, diamonds) and free energies ($G(H_2O)$, triangles) in aqueous solution for a few low-energy $Cu^{2+}\cdots$bitucarpin A complexes. The relative potential energy in vacuo (ΔE(vac), down triangles) is also displayed.

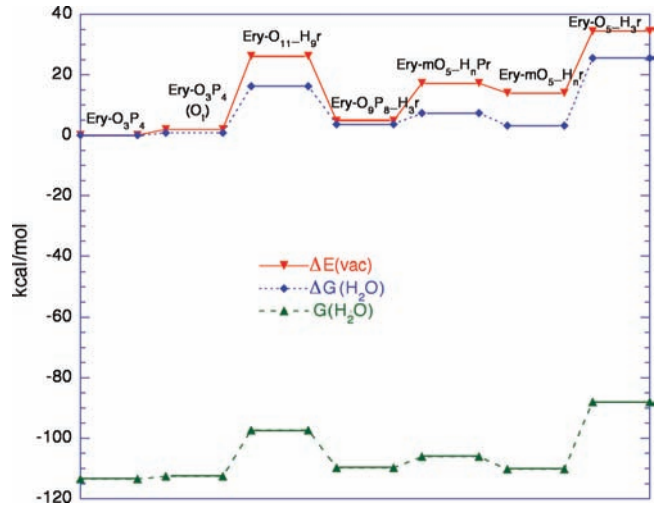

Figure 4. IEF-PCM/B3LYP/6-31G* relative free energies ($\Delta G(H_2O)$, diamonds) and free energies ($G(H_2O)$, triangles) in aqueous solution for a few low-energy $Cu^{2+}\cdots$erybraedin C complexes. The relative potential energy in vacuo (ΔE(vac), down triangles) is also displayed.

This is the case for coordination sites of the cation in the O_{11} region (G_{sol}(def) = −123 and −120 kcal/mol, for **Bit-O$_{11}$** and **Bit-O$_{11}$_r**, respectively), followed by **Bit-m2_r** (G_{sol}(def) = −117 kcal/mol) where the cation is bridged between the ring D and O_5, but freely accessible through a wide solid angle. An intermediate situation occurs when Cu^{2+} is monodentate to the O lp (**Bit-OMe**, G_{sol}(def) = −114 kcal/mol) or chelated within the D ring of the scaffold and the prenyl group (G_{sol}(def) = −117 and −114 kcal/mol), whereas the minimum (yet large) solvent effect is found when the cation is bound to the prenyl group moiety and the methoxy O lone pairs (**Bit-OP**, G_{sol}(def) = −109 kcal/mol), irrespective of the scaffold arrangement (**Bit-OP (O$_t$)**, G_{sol}(def) = −110 kcal/mol), as can be inferred also from the data reported in Table 7. Interested readers can find the absolute values (E_h) in aqueous solution (IEF-PCM) as well as a variety of relative energies and free energies (kcal/mol) in Table S3 of the Supporting Information.

Concerning the MIA in solution, the main difference with respect to the gas phase, brought out when the complex structure is embedded in solution and allowed to relax, is a significant decrease in the affinity value (by 36−158 kcal/mol), again depending on the extension of the ion surface exposed to the solvent, and thus on the solvent competition with the ligand. The correlation between the gas phase and solution values therefore is roughly linear only within each set of coordination complexes considered, but due to the variety of sites taken into account, the relevant plots are scarcely populated. Actually a systematic study of the full set of complexes is prevented by the large size of the systems considered and by the computational cost of geometry optimizations in solution, whose convergence in addition is remarkably difficult to attain. An analogous trend is obtained also for erybraedin C.

2. Erybraedin C. The solvent effect dampens the free energy differences for erybraedin C, significantly stabilizing the coordination complexes with the metal cation most exposed to the solvent, as already pointed out for bitucarpin A, that on an average have a lower stability in vacuo. As can be derived from the plots displayed in Figure 4 and from the values reported in Table 8, the stabilities of **Ery-O$_3$P$_4$** (irrespective of the scaffold arrangement) and **Ery-O$_9$P$_8$_H$_3$r** remain almost unaltered with respect to those in the gas phase (G_{sol}(def) ≈ −114 kcal/mol). Conversely, the chelated structures of the **Ery-mO$_5$** type as well as **Ery-O$_{11}$_H$_9$r** resent a similar, and beneficial, solvent effect (G_{sol}(def) ≈ −123 kcal/mol).

Interestingly enough, the MIA in solution for the sequestered structures remains significantly favorable, decreasing by a limited amount (8−26 kcal/mol). Absolute values (E_h) as well as a variety of relative energies and free energies (kcal/mol) can be found in Table S4 of the Supporting Information.

The solvent effect on the cation charge and on the donor−acceptor interactions is not reported because they are fairly consistent with those of plicatin B, discussed in our previous article.[12]

Let us compare the coordination behavior of bitucarpin A and erybraedin C with that of plicatin B, considered a very effective antioxidant,[32,33] although Rosa et al.[13] concluded that, in this series, erybraedin C qualifies as the most interesting antioxidant, deserving further investigations in vivo.

D. Comparison among the MIA of the Two Pterocarpans and Plicatin B. As already mentioned, both bitucarpin A and erybraedin C feature a fused ring scaffold that allows limited flexibility to the structure (H_t to O_t interconversion), beside *R*,*R* and *R*,*S* configurations, the latter being significantly less stable than the former.[11] Conversely, plicatin B shows a variety of rotamers, *E* and *Z* configurations on the α,β unsaturated ester side chain, keto tautomers, and fused ring isomers available that produced more than 100 different complexes with Cu^{2+}.[12] This fact suggested that its potency might derive from the wide opportunity of binding Cu^{2+} offered by plicatin B, whatever structure it takes under such environmental conditions. Despite the fact that at this computational level plicatin has just 310

basis functions, whereas bitucarpin and erybraedin dimensions are 434 and 484 atomic orbitals, respectively, a large variety of starting conformations have been considered also for them, that however eventually produced "only" 13 and 22 different complexes, respectively. As already stated, the scan of torsion angles has been performed only in a limited number of cases to identify the most stable structures and evaluate their MIA in vacuo and in solution, further exploring the most convenient ones.

The preferred binding sites of Cu^{2+} on the conserved locations (vicinal prenyl and OH groups) are fairly similar in erybraedin C and plicatin B. In contrast, the presence of the ester head supplies an additional site to plicatin B, especially in the anti arrangement of the carboxy OMe. The reducing properties of plicatin B toward Cu(II) are analogous to those of bitucarpin and erybraedin. In order to assess the role of its side chains, two distinct copper···plicatin B complexes, **8a_E** and **8a_PO**, have been considered, replacing their prenyl (in **8a_E**) and α,β-unsaturated methyl ester (in **8a_PO**) side chains, respectively, with a H. The Cu spin density turned out to be 0.005 and 0.004, respectively, while the MIA decreased from 343 to 319.30 kcal/mol (E_{def} = 7.65 kcal/mol) and from 334.85 to 304.02 kcal/mol (E_{def} = 10.25 kcal/mol). Interestingly enough, the bare phenol obtained by replacing also the prenyl group with an H in **8a_PO-ester** maintained the reducing properties (Cu spin density = 0.003), albeit with a sharp decrease in the MIA, that dropped to 246.55 kcal/mol.

The most favorable binding sites are found for the *Z* configurations and the keto tautomers: their MIA however suffers a significant decrease (>80 kcal/mol) in solution. The MIA in vacuo is somewhat more favorable for bitucarpin A and erybraedin C than for plicatin B, with the best value found for erybraedin. In aqueous solution a limited decrease in the MIA is computed for erybraedin C, whose best value is 360 kcal/mol, whereas that observed for bitucarpin A is remarkably large (just two structures stop soon, ending their fall at 327 kcal/mol). Therefore, taking into account only the most favorable values, the MIA ordering is erybraedin C > bitucarpin A > plicatin B both in vacuo and in aqueous solution. This ordering should also correspond to their antioxidant activity.

E. Conclusions

A large number of complexes with Cu^{2+} of bitucarpin A and erybraedin C have been considered in vacuo at the B3LYP/6-31G* level, with the open shell dication described using pseudopotentials coupled with the LanL2DZ valence basis set. The energy refinement produced however a limited number of stable complexes, because several distinct initial structures ended into the same basin, corresponding to a single coordination complex, with the Cu(II) cation reduced to Cu(I) and the ligand oxidized to a radical cation. The metal ion affinity (MIA) for bitucarpin A and erybraedin C turns out to be very favorable in vacuo (at most 371 and 380 kcal/mol, respectively, with the cation dentated between the prenyl π density and the O lone pairs or the D ring). The continuum solvent in the IEF-PCM framework hardly affects structure and stability but dampens the free energy differences. Conversely, the MIA (tentatively evaluated in solution employing the entire cavity for each rigid partner in turn) decreases to 327 and 360 kcal/mol, respectively.

The nature of the stable complexes earlier located for plicatin B shows a remarkable variety with respect to bitucarpin A and erybraedin C, with structures of *Z* configuration more favorably coordinated (357−343 kcal/mol) and preferentially solvated. Their number is much larger as well. The solvent effect on plicatin B significantly reduces the MIA (by 85−150 kcal/mol) that turns out to be 265 kcal/mol, at most, in solution. Therefore, from the present investigation, erybraedin C is expected to be the most effective natural antioxidant in this series, followed by bitucarpin A, whereas plicatin B, despite the wealth of active rotamers/tautomers available, remains further apart from the two pterocarpans. Progressive elimination of its side chains, however, does not affect its reducing character toward Cu(II) but makes the MIA decrease significantly.

Unfortunately, homogeneous experimental data are not available, because only plicatin B was considered in ref 32 while bitucarpin A was disregarded (because was not active during linoleic acid autoxidation) in ref 13, the experimental investigation that assigns a much higher antioxidant activity to erybraedin C than to plicatin B. NPA charges and Mulliken spin densities, however, clearly support the antioxidant character of all the ligands considered here that, besides sequestering the cation, reduce it thus preventing its oxidative action on LDL.

Supporting Information Available: Tables of labels, structures, and absolute energies of bitucarpin A···Cu^{2+} complexes in vacuo and erybraedin C···Cu^{2+} complexes in vacuo, detailed discussions on the structures of the complexes, tables of labels, structures, and absolute energies of bitucarpin A···Cu^{2+} complexes in solution and erybraedin C···Cu^{2+} complexes in solution, and NPA/NBO extracts from Gaussian outputs, NBO analysis of the bonding. This information is available free of charge via the Internet at http://pubs.acs.org.

References and Notes

(1) Dewick, P. M. In *The Flavonoids, Advances in Research Since 1986*; Harborne, J. B., Ed.; Chapman & Hall: London, U.K., 1994; pp 166−180.
(2) Dewick, P. M.; Steel, M. J. *Phytochemistry* **1982**, *21*, 1599–1603.
(3) Lane, G. A.; Sutherland, O. R. W.; Skipp, A. R. *J.Chem. Ecol.* **1987**, *13*, 771–783.
(4) Perrin, D. R.; Cruickshank, I. A. M. *Phytochemistry* **1969**, *8*, 971–978.
(5) Nakagawa, M.; Nakanishi, K.; Darko, L. L.; Vick, J. A. *Tetrahedron Lett.* **1982**, *23*, 3855–3858.
(6) Engler, T. A.; Lynch, K. O., Jr.; Reddy, J. P.; Gregory, G. S. *Bioorg. Med. Chem. Lett.* **1993**, *3*, 1229–1232.
(7) Engler, T. A.; LaTessa, K. O.; Reddy, J. P.; Iyengar, R.; Chai, W.; Agrios, K. *Bioorg. Med. Chem.* **1996**, *4*, 1755–1769.
(8) Lee, J. H.; Lee, B. W.; Kim, J. H.; Jeong, T.-S.; Kim, M. J.; Lee, W. S.; Park, K. H. *J. Agric. Food Chem.* **2006**, *54*, 2057–2063.
(9) Steinberg, D.; Pathasarathy, S.; Carew, T. E.; Khoo, J. C.; Witztum, J. L. *N. Engl. J. Med.* **1989**, *320*, 915–924.
(10) Daugherty, A.; Roselaar, S. E. *Cardiovasc. Res.* **1995**, *29*, 297–311.
(11) Alagona, G.; Ghio, C.; Monti, S. *Phys. Chem. Chem. Phys.* **2004**, *6*, 2849–2857.
(12) Alagona, G.; Ghio, C. *Phys. Chem. Chem. Phys.* **2009**, *11*, 776–790.
(13) Rosa, A.; Deiana, M.; Corona, G.; Atzeri, A.; Incani, A.; Appendino, G.; Dessì, M. A. *Eur. J. Lipid Sci. Technol.* **2005**, *107*, 521–529.
(14) (a) Becke, A. D. *J. Chem. Phys.* **1993**, *98*, 5648–5652. (b) Lee, C.; Yang, W.; Parr, R. G. *Phys. Rev. B* **1988**, *37*, 785–789.
(15) (a) Ditchfield, R.; Hehre, W. J.; Pople, J. A. *J. Chem. Phys.* **1971**, *54*, 724–728. (b) Hehre, W. J.; Ditchfield, R.; Pople, J. A. *J. Chem. Phys.* **1972**, *56*, 2257–2261. (c) Dill, J. D.; Pople, J. A. *J. Chem. Phys.* **1975**, *62*, 2921–2923. (d) Hariharan, P. C.; Pople, J. A. *Theor. Chim. Acta* **1973**, *28*, 213–222.
(16) Frisch, M. J.; Trucks, G. W.; Schlegel, H. B.; Scuseria, G. E.; Robb, M. A.; Cheeseman, J. R.; Montgomery, J. A., Jr.; Vreven, T.; Kudin, K. N.; Burant, J. C.; Millam, J. M.; Iyengar, S. S.; Tomasi, J.; Barone, V.; Mennucci, B.; Cossi, M.; Scalmani, G.; Rega, N.; Petersson, G. A.; Nakatsuji, H.; Hada, M.; Ehara, M.; Toyota, K.; Fukuda, R.; Hasegawa, J.; Ishida, M.; Nakajima, T.; Honda, Y.; Kitao, O.; Nakai, H.; Klene, M.; Li, X.; Knox, J. E.; Hratchian, H. P.; Cross, J. B.; Bakken, V.; Adamo, C.; Jaramillo, J.; Gomperts, R.; Stratmann, R. E.; Yazyev, O.; Austin, A. J.; Cammi, R.; Pomelli, C.; Ochterski, J. W.; Ayala, P. Y.; Morokuma, K.; Voth, G. A.; Salvador, P.; Dannenberg, J. J.; Zakrzewski, V. G.; Dapprich, S.; Daniels, A. D.; Strain, M. C.; Farkas, O.; Malick, D. K.; Rabuck, A. D.;

Raghavachari, K.; Foresman, J. B.; Ortiz, J. V.; Cui, Q.; Baboul, A. G.; Clifford, S.; Cioslowski, J.; Stefanov, B. B.; Liu, G.; Liashenko, A.; Piskorz, P.; Komaromi, I.; Martin, R. L.; Fox, D. J.; Keith, T.; Al-Laham, M. A.; Peng, C. Y.; Nanayakkara, A.; Challacombe, M.; Gill, P. M. W.; Johnson, B.; Chen, W.; Wong, M. W.; Gonzalez, C.; and Pople, J. A. *Gaussian 03, Revision C.02*; Gaussian, Inc.: Wallingford, CT, 2004.

(17) Hay, P. J.; Wadt, W. R. *J. Chem. Phys.* **1985**, *82*, 270–283.

(18) (a) de Bruin, T. J. M.; Marcelis, A. T. M.; Zuilhof, H.; Sudhölter, E. J. R. *Phys. Chem. Chem. Phys.* **1999**, *1*, 4157–4163. (b) Kaneti, J.; de Smet, L. C. P. M.; Boom, R.; Zuilhof, H.; Sudhölter, E. J. R. *J. Phys. Chem. A* **2002**, *106*, 11197–11204.

(19) Ruiz, E.; Cirera, J.; Alvarez, S. *Coord. Chem. Rev.* **2005**, *249*, 2649–2660.

(20) Marino, T.; Russo, N.; Toscano, M. *J. Mass Spectrom.* **2002**, *37*, 786–791.

(21) (a) Miertus, S.; Scrocco, E.; Tomasi, *J. Chem. Phys.* **1981**, *55*, 117–129. (b) Miertus, S.; Tomasi, *J. Chem. Phys.* **1982**, *65*, 239–245. (c) Tomasi, J.; Persico, M. *Chem. Rev.* **1994**, *94*, 2027–2094. (d) Tomasi, J.; Mennucci, B.; Cammi, R. *Chem. Rev.* **2005**, *105*, 2999–3094.

(22) (a) Foster, J. P.; Weinhold, F. *J. Am. Chem. Soc.* **1980**, *102*, 7211–7218. (b) Carpenter, J. E.; Weinhold, F. *J. Mol. Struct.: THEOCHEM* **1988**, *169*, 41–62.

(23) (a) Reed, A. E.; Weinhold, F. *J. Chem. Phys.* **1983**, *78*, 4066–4073. (b) Reed, A. E.; Weinstock, R. B.; Weinhold, F. *J. Chem. Phys.* **1985**, *83*, 735–746.

(24) Becke, A. D. *J. Chem. Phys.* **1993**, *98*, 1372–1377.

(25) Poater, J.; Solà, M.; Rimola, A.; Rodríguez-Santiago, L.; Sodupe, M. *J. Phys. Chem. A* **2004**, *108*, 6072–6078.

(26) Alagona, G.; Ghio, C. *J. Phys. Chem. A* **2006**, *110*, 647–659.

(27) Rice-Evans, C. In *Antioxidant Food Supplements in Human Health*; Packer, L., Hiramatsu, M., Yoshikawa, T., Eds.; Academic Press: San Diego, CA, 1999; pp 239−253.

(28) (a) Miranda, C. L.; Stevens, J. F.; Ivanov, V.; McCall, M.; Frei, B.; Deinzer, M. L.; Buhler, D. R. *J. Agric. Food Chem.* **2000**, *48*, 3876–3884. (b) Stevens, J. F.; Miranda, C. L.; Frei, B.; Buhler, D. R. *Chem. Res. Toxicol.* **2003**, *16*, 1277–1286.

(29) (a) Lamsabhi, A. M.; Alcamí, M.; Mó, O.; Yáñez, M.; Tortajada, J. *ChemPhysChem* **2004**, *5*, 1871–1878. (b) Lamsabhi, A. M.; Alcamí, M.; Mó, O.; Yáñez, M.; Tortajada, J.; Salpin, J.-Y. *ChemPhysChem* **2007**, *8*, 181–187.

(30) Alagona, G.; Ghio, C.; Monti, S. *J. Phys. Chem. B* **2005**, *109*, 16918–16925.

(31) Noguera, M.; Bertran, J.; Sodupe, M. *J. Phys. Chem. A* **2005**, *108*, 333–341.

(32) Baldi, S.; Maurich, T.; Lubrano, V.; Turchi, G. In *Proceedings of the 8th International Conference on Mechanisms of Antimutagenesis and Anticarcinogenesis, Pisa, Italy, 2003*; Bronzetti, G., Ferguson, L. R., De Flora, S., Eds.; 2003; p 14.

(33) Lubrano, V.; Boni, G.; L'Abbate, A.; Turchi, G. *Drug Chem. Toxicol.* **2007**, *30*, 311–325.

JP905521U